DOI: 10.1021/ic900677c

Inorganic Chemistry
Article

Mononuclear Platinum(II) Complexes Incorporating κ^2-Carboxylate Ligands: Synthesis, Structure, and Reactivity

Marc-Etienne Moret, Sebastian F. Keller, J. Chris Slootweg,† and Peter Chen*

Laboratorium für Organische Chemie, Eidgenössische Technische Hochschule (ETH) Zürich, CH-8093 Zürich, Switzerland. †Present address: Department of Chemistry and Pharmaceutical Sciences, Vrije Universiteit Amsterdam, De Boelelaan 1083, 1081 HV Amsterdam, The Netherlands

Received April 7, 2009

The chloro-bridged dimer $[(PC)Pt(\mu\text{-}Cl)]_2$ ($PC = [(^tBu_2P\text{-}o\text{-}C_6H_4)\text{-}CMe_2]^-$) reacts with silver(I) acetate to yield the monomeric κ^2-acetate complex $[(PC)Pt(\kappa^2\text{-}OOCMe)]$. Its trifluoroacetate analogue exists in solution as a mixture of the monomer and two isomeric dimers, and crystallizes as the approximately C_2-symmetrical dimer $[(PC)Pt(\mu\text{-}OOCCF_3)]_2$. NMR experiments and density functional theory calculations show that the monomeric species are favored by bulky ligands and electron-rich carboxylates. $[(PC)Pt(OOCCF_3)]$ undergoes a ligand-dehydrogenation reaction in hot trifluoroacetic acid to yield $[(PCC)Pt(OOCCF_3)_2]$ ($PCC = (^tBu_2P\text{-}o\text{-}C_6H_4)\text{-}C(Me)=CH_2$).

Introduction

Carboxylate complexes of Group 10 metals have received a lot of attention in the last decades because of their widespread use in catalysis. For example, palladium acetate complexes with various donor ligands are efficient catalyst precursors for a range of cross-coupling reactions[1−5] and oxidative functionalization of C−H bonds,[6] and palladium trifluoroacetate is able to catalyze the oxidative dehydrogenation of cyclic olefins to yield aromatic compounds.[7,8] Platinum acetate[9] and trifluoroacetate[10,11] complexes are active benzene deuteration catalysts, and there is evidence[10,12] that these reactions proceed via heterolytic C−H activation, whereby the carboxylate ligand is pivotal and acts as an internal base.

Scheme 1

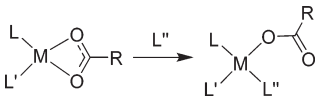

To allow efficient catalyst tuning a good knowledge of the available structures in solution and their dynamics is essential.[13,14] Of particular interest are mononuclear Pd(II) and Pt(II) complexes of general formula $[LL'M(\kappa^2\text{-}OOCR)]^{n+}$ (where L and L′ are σ-donor ligands; $n = 0$ or 1), which, in principle, are ready to accommodate an incoming ligand by opening the 4-membered M−O−C−O chelate (Scheme 1). These κ^2-acetate complexes have been postulated as intermediates in catalytic cycles[4,5,9] and observed in solution at high dilution,[15] but structurally characterized species are exceedingly rare, with, to our knowledge, only three examples for Pd(II)[13,16,17] and one for Pt(II).[18] This lacuna in coordination chemistry is mainly due to the high propensity of

*To whom correspondence should be addressed. E-mail: peter.chen@org.chem.ethz.ch.

(1) Beletskaya, I. P.; Cheprakov, A. V. *J. Organomet. Chem.* **2004**, *689*, 4055–4082.
(2) Farina, V. *Adv. Synth. Catal.* **2004**, *346*, 1553–1582.
(3) Giumanini, A. G.; Chiavari, G.; Musiani, M. M.; Rossi, P. *Synthesis* **1980**, *9*, 743–746.
(4) Herrmann, W. A.; Brossmer, C.; Reisinger, C.-P.; Riermeier, T. H.; Öfele, K.; Beller, M. *Chem.—Eur. J.* **1997**, *3*, 1357–1364.
(5) Herrmann, W. A.; Brossmer, C.; Öfele, K.; Reisinger, C.-P.; Piermeier, T.; Beller, M.; Fischer, H. *Angew. Chem., Int. Ed. Engl.* **1995**, *34*, 1844–1848.
(6) Dick, A. R.; Sanford, M. S. *Tetrahedron* **2006**, *62*, 2439–2463.
(7) Trost, B. M.; Metzner, P. J. *J. Am. Chem. Soc.* **1980**, *102*, 3572–3577.
(8) Bercaw, J. E.; Hazari, N.; Labinger, J. A. *J. Org. Chem.* **2008**, *73*, 8654–8657.
(9) Gerdes, G.; Chen, P. *Organometallics* **2004**, *23*, 3031–3036.
(10) Young, K. J. H.; Meier, S. K.; Gonzales, J. M.; Oxgaard, J.; Goddard, W. A. III; Periana, R. A. *Organometallics* **2006**, *25*, 4734–4737.
(11) Ziatdinov, V. R.; Oxgaard, J.; Mironov, O. A.; Young, K. J. H.; Goddard, W. A. III; Periana, R. A. *J. Am. Chem. Soc.* **2006**, *128*, 7404–7405.
(12) Biswas, B.; Sugimoto, M.; Sakaki, S. *Organometallics* **2000**, *19*, 3895–3908.
(13) Thirupathi, N.; Amoroso, D.; Bell, A.; Protasiewicz, J. D. *Organometallics* **2005**, *24*, 4099–4102.
(14) Thirupathi, N.; Amoroso, D.; Bell, A.; Protasiewicz, J. D. *Organometallics* **2007**, *26*, 3157–3166.
(15) Fiddy, S. G.; Evans, J.; Newton, M. A.; Neisius, T.; Tooze, R. P.; Oldman, R. *Chem. Commun.* **2003**, 2682–2683.
(16) Viciu, M. S.; Stevens, E. D.; Petersen, J. L.; Nolan, S. P. *Organometallics* **2004**, *23*, 3752–3755.
(17) Lee, J.-C.; Wang, M.-G.; Hong, F.-E. *Eur. J. Inorg. Chem.* **2005**, 5011–5017.
(18) Bigeault, J.; Giordano, L.; de Riggi, I.; Guimbert, Y.; Buono, G. *Org. Lett.* **2007**, *9*, 3567–3570.

Published on Web 06/23/2009

Scheme 2

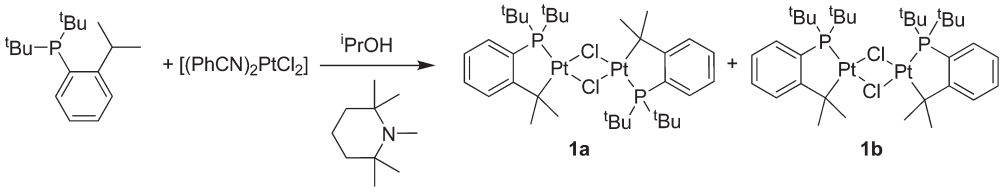

such complexes to form dimeric, carboxylate-bridged structures[19−28] that are, most probably, less active in catalysis.

We here present the synthesis and characterization of neutral platinum(II) complexes incorporating a bulky, cyclometalated phosphine donor and a κ^2-acetate or trifluoroacetate ligand. The factors that govern the monomer−dimer equilibrium are treated on the basis of solution-phase NMR measurements and density functional theory (DFT) calculations. Finally, we report that the trifluoroacetate complex undergoes an acceptor-free ligand-dehydrogenation process in hot trifluoroacetic acid.

Results and Discussion

Complex Synthesis. The dimeric, chloro-bridged platinacycle $[(PC)Pt(\mu\text{-}Cl)]_2$ (**1**, PC = $[(^tBu_2P\text{-}o\text{-}C_6H_4)\text{-}CMe_2^-]$) was synthesized by a modification of the procedure by Shaw and co-workers,[29] whereby 1,2,2,6,6-pentamethylpiperidine was used instead of excess phosphine to trap the formed HCl (Scheme 2). In contrast with the original report, we obtained **1** as a 3:2 mixture of two isomers, which were ascribed to structures **1a** and **1b** (Scheme 2).

Reaction of compound **1** with silver acetate yielded the mononuclear complex **2a** (Scheme 3), which was structurally characterized by X-ray diffraction (XRD, Figure 1). The coordination around the platinum center is best described as a distorted square plane, with bite angles of 86° and 60° for the PC and acetate ligands, respectively. As expected from the stronger *trans* influence of the alkyl ligand, the Pt1−O1 (2.230 Å) bond is markedly longer than Pt1−O2 (2.170 Å), the latter being comparable with the Pt−O distance of 2.166 Å found in $\{[(^tBu)(Ph)PO]_2H\}$-Pt(κ^2-OOCMe).[18]

In contrast, reaction of **1** with silver trifluoroacetate afforded after crystallization dimer **3b**, as was determined unequivocally by XRD (Figure 2). The structure of **3b** has

Scheme 3

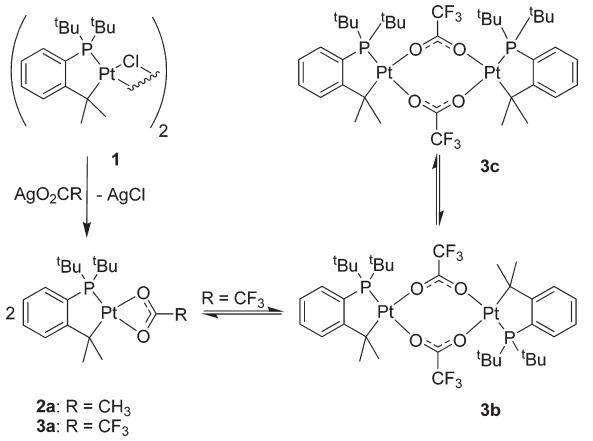

approximate C_2 symmetry, with each bridging trifluoroacetate unit being *trans* to one phosphorus and one carbon atom. Considering the Pt−O−C−O dihedral angle (hereafter called α), the coordination mode of a carboxylate ligand can be described as *syn* (α = 0), *anti* (α = 180°), or *skew* (α = ±90°).[30] **3b** exhibits α angles of 1° and −9° *trans* to the phosphorus atom, and of −35° and −50° *trans* to the carbon atom. Thus, the coordination of the bridging CF_3COO^- ligands is intermediate between *syn-syn* and *syn-skew*. The Pt−O−C angles (hereafter called *β*), ranging from 134.5° to 137.4°, differ significantly from the ideal angle of 120° expected from sp^2 hybridization of the carboxylate oxygen, which implies a profound distortion of the central ring.

The solution phase behavior of **2** and **3** was investigated by multinuclear NMR spectroscopy. The ^1H, ^{13}C, and ^{31}P NMR spectra of **2** are consistent with the presence of monomeric **2a** as sole species. Interestingly, long-range $^{13}C-^{31}P$ couplings are observed for all carbon nuclei, including those of the acetate ligand ($^3J(C-P)$ = 3.2 Hz and $^4J(C-P)$ = 2.8 Hz), which is likely due to the rigid, planar structure of the complex.

The situation is more complex for the trifluoroacetate analogue **3**. At room temperature, the ^{19}F and ^{31}P spectra display two broad signals each, indicating the presence of two main species in solution, which we attribute to monomer **3a** and dimer **3b**. The ratio between these species depends on the concentration (Figure 3), which is indicative for the existence of a monomer−dimer equilibrium.

More detailed information about the speciation of **3** in solution was obtained by variable temperature NMR spectroscopy. ^{19}F NMR spectra recorded at temperatures ranging from −50 to 30 °C are plotted in Figure 4.

(19) Slootweg, J. C.; Chen, P. *Organometallics* **2006**, *25*, 5863–5869.
(20) Powell, J.; Jack, T. *Inorg. Chem.* **1972**, *11*, 1039–1048.
(21) Butikofer, J. L.; Hoerter, J. M.; Peters, R. G.; Roddick, D. M. *Organometallics* **2004**, *23*, 400–408.
(22) Cooper, M. K.; Guerney, P. J.; Goodwin, H. J.; McPartlin, M. *J. Chem. Soc., Dalton Trans.* **1982**, 757–764.
(23) Miyamoto, T. K.; Ichida, H. *Bull. Chem. Soc. Jpn.* **1991**, *64*, 1835–1839.
(24) Navarro-Ranniger, C.; López-Solera, I.; Pérez, J. M.; Rodríguez, J.; García-Ruano, J. L.; Raithby, P. R.; Masaguer, J. R.; Alonso, C. *J. Med. Chem.* **1993**, *36*, 3795–3801.
(25) Newkome, G. R.; Theriot, K. J.; Fronczek, F. R.; Villar, B. *Organometallics* **1989**, *8*, 2513–2523.
(26) Sasai, K.; Takeshita, M.; Tanaka, Y.; Ue, T.; Yanagisawa, M.; Kosaka, M.; Tsubomura, T.; Ato, M.; Nakano, T. *J. Am. Chem. Soc.* **1998**, *120*, 11353–11363.
(27) Cheney, A. J.; Shaw, B. L. *J. Chem. Soc., Dalton Trans.* **1972**, 754–763.
(28) Jain, V. K.; Jain, L. *Coord. Chem. Rev.* **2005**, *249*, 3075–3197.
(29) Gill, D.; Mann, B. E.; Shaw, B. L. *J. Chem. Soc., Dalton Trans.* **1973**, 270–278.
(30) Cotton, F. A.; Wilkinson, G.; Murillo, C. A.; Bochman, M. *Advanced Inorganic Chemistry*, 6th ed.; John Wiley & Sons: New York, 1999.

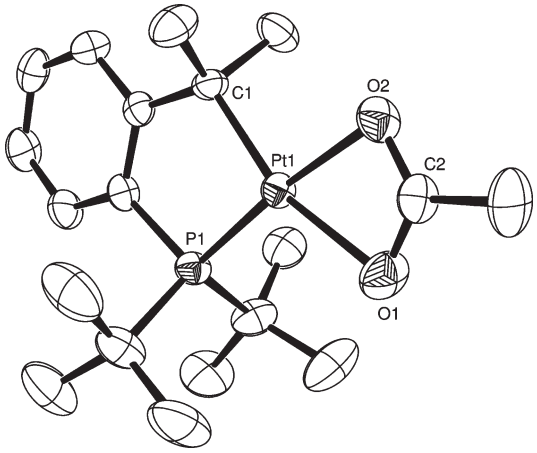

Figure 1. Oak Ridge thermal ellipsoid plot (ORTEP) representation of the X-ray crystal structure of **2a**. Ellipsoids are drawn at 50% probability. Selected distances [Å], angles [deg]: Pt1−C1 2.043(4), Pt1−P1 2.1741(9), Pt1−O2 2.170(2), Pt1−O1 2.230(3), C2−O2 1.260(4), C2−O1 1.267(5), C1−Pt1−P1 85.87(10), C1−Pt1−O2 100.79(12), O2−Pt1−O1 59.59 (10), P1−Pt1−O1 113.74(8), Pt1−O2−C2 88.8(2), Pt1−O1−C2 91.7(2).

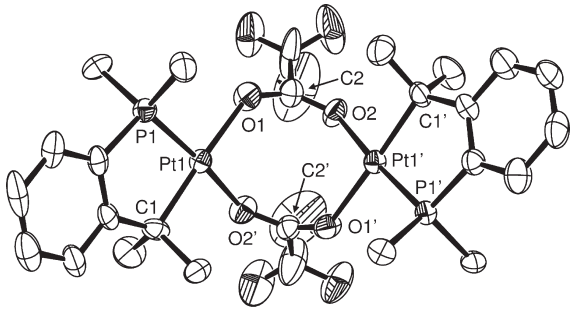

Figure 2. ORTEP representation of the X-ray crystal structure of **3b**. Ellipsoids are drawn at 50% probability. For clarity, only the central carbon of *tert*-butyl substituents is plotted. Selected distances [Å], angles [deg], and dihedral angles [deg] (values for the approximate C_2 symmetry equivalents given in square parentheses): Pt1−C1 2.067(9) [2.060(10)], Pt1−P1 2.190(2) [2.191(2)], Pt1−O1 2.202(7) [2.206(7)], Pt1−O2′ 2.138(7) [2.154(7)], O1−C2 1.225(12) [1.195(12)], O2−C2′ 1.228(12) [1.222(12)], P1−Pt1−C1 87.4(3) [87.0(3)], P1−Pt1−O1 98.9(2) [98.75(19)], C1−Pt1−O2′ 87.9(4) [90.2(3)], O1−Pt1−O2′ 83.6(3) [83.8(3)], Pt1−O1−C2 136.0(7) [135.1(7)], Pt1−O2′−C2′ 134.5(7) [137.4(7)], O1−C2−O2 133.6(11) [133.8(10)], P1−Pt1−O1−C2 154.8(11) [169(11)], C1−Pt1−O2′−C2′ −106.1(11) [−105.4(12)], Pt1−O1−C2−O2 −35(2) [−50(2)], Pt1−O2′−C2′−O1′ 1(2) [−9(2)].

At −50 °C, the signal at δ −74.3 ppm accounts for about 80% of the spectrum, and three weaker resonances are observed at −74.1, −74.6, and −75.4 ppm. Upon gradually increasing the temperature, the signal at −75.4 ppm broadens and disappears above −10 °C. All other resonances broaden as well and a new, broad signal at −74.8 ppm becomes the most intense signal at $T = 30$ °C.

These results are interpreted as follows: following the principle of Le Châtelier, the signal at −74.8 ppm, which is favored at higher temperatures and high dilution, is attributed to the monomer **3a** (Scheme 3). The resonance at −74.3 ppm is assigned to the dimer **3b**, in which both CF_3COO^- units are equivalent. Dimer **3c**, with two nonequivalent CF_3COO^- ligands, should give rise to two different ^{19}F signals. Assuming that the ^{19}F chemical shift in these complexes is mainly affected by inductive effects due to *trans*-influence, the two signals of **3c** should be found on either side of the resonance for **3b**. Thus, the

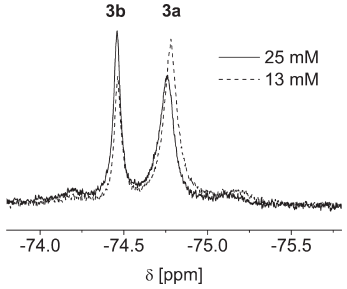

Figure 3. ^{19}F NMR spectra of **3** recorded at room temperature at two different concentrations in CD_2Cl_2. Peak integration indicates **3a**/**3b** ratios of 57:43 and 70:30 at total concentrations of 25 and 13 mM, respectively.

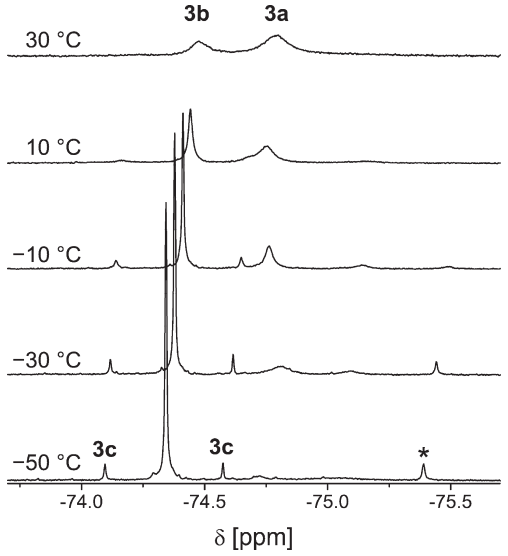

Figure 4. ^{19}F NMR spectra of **3** (25 mM in CD_2Cl_2) recorded at different temperatures. Peak integration indicates a **3c**/**3b** ratio of about 1:9 at −50 °C. The peak marked with * is tentatively assigned to a higher oligomer.

signals at −74.1 and −74.6 ppm are attributed to dimer **3c**. The signal at −75.4 ppm is tentatively assigned to a higher oligomer of **3**, in accord with the fact that it disappears above −10 °C.

DFT Calculations. To support our interpretation of the experimental data, we investigated all possible structures of **2** and **3** (Chart 1) by means of DFT calculations. The geometries of structures **2a**−**c** and **3a**−**c** were optimized at the B3PW91 level with the SDD pseudopotential and basis functions on platinum and 6-31G(d) on all other atoms. For comparison, we also analyzed the geometries of the model complexes **4a**−**c** and **5a**−**c** (Chart 1), where the *tert*-butyl groups on the phosphorus atom and the methyl groups on the platinum-bound carbon atom have been replaced by hydrogen atoms. For each dimer, we computed the dimerization energy ΔE_{dim} defined as follows:

$$\Delta E_{dim} = (1/2)E_{dimer} - E_{monomer}$$

where E_{dimer} and $E_{monomer}$ are the corresponding energies computed at 0 K (Table 1).

The minute dimerization energies computed for **2b** (0.02 kcal/mol) and **2c** (0.25 kcal/mol) are consistent with

Chart 1

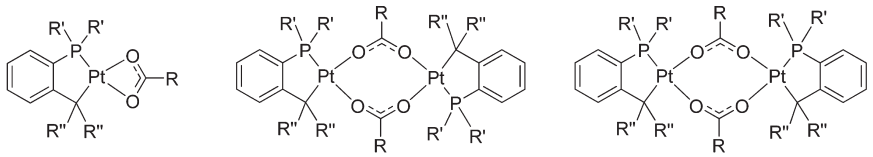

2a: R = CH_3, R' = t-Bu, R'' = CH_3
3a: R = CF_3, R' = t-Bu, R'' = CH_3
4a: R = CH_3, R' = R'' = H
5a: R = CF_3, R' = R'' = H

2b-5b **2c-5c**

Table 1. Computed Dimerization Energies ΔE_{dim} (per Monomer Unit) and Intramolecular Pt−Pt Distances for Compounds **2**−**5**

structure	ΔE_{dim} [kcal/mol]	Pt−Pt [Å]	RCOO binding mode	$\langle\beta\rangle$ [deg][a]
2b	0.02	4.656	*syn-skew*	122.2
2c	0.25	4.606	*syn-skew*	122.2
3b	−4.12	4.322	*syn-syn/skew*[b]	132.0
3c	−4.37	4.714	*syn-skew*	124.4
4b	−9.49	3.066	*syn-syn*	126.0
4c	−9.10	3.093	*syn-syn*	126.5
5b	−12.99	3.133	*syn-syn*	125.7
5c	−12.67	3.164	*syn-syn*	126.1

[a] β: Pt−O−C angle. [b] The Pt−O−C−O dihedral angles have values of −7.1° and −60.8°.

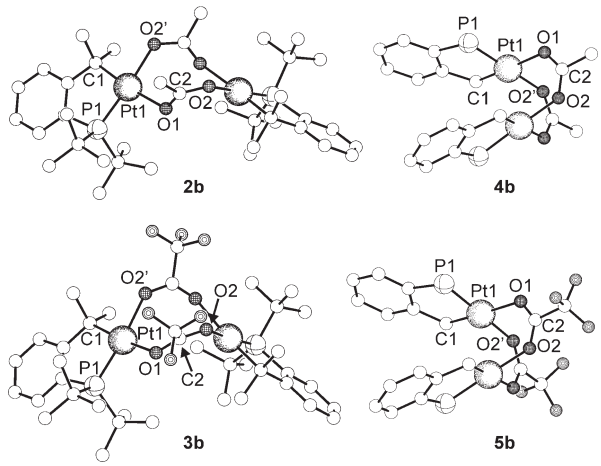

Figure 5. Computed structures for dimers **2b**−**5b**. Hydrogen atoms are excluded for clarity. All optimizations were performed without symmetry constraints, but no significant differences between C_2 symmetry equivalent parameters were found. Selected distances [Å], angles [deg], and dihedral angles [deg] **2b**: Pt1−C1 2.065, Pt1−P1 2.223, Pt1−O1 2.240, Pt1−O2′ 2.146, Pt1−Pt1′ 4.656, O1−Pt1−O2′ 84.1, Pt1−O1−C2 122.4, Pt1−O2′−C2′ 122.0, P1−Pt1−O1−C2 −144.7, C1−Pt1−O2′−C2′ −127.4, Pt1−O1−C2−O2 −115.0, Pt1−O2′−C2′−O1′ 11.7. **3b**: Pt1−C1 2.067, Pt1−P1 2.224, Pt1−O1 2.235, Pt1−O2′ 2.149, Pt1−Pt1′ 4.322, O1−Pt1−O2′ 85.1, Pt1−O1−C2 133.0, Pt1−O2′−C2′ 130.9, P1−Pt1−O1−C2 176.5, C1−Pt1−O2′−C2′ −106.7, Pt1−O1−C2−O2 −60.8, Pt1−O2′−C2′−O1′ −7.1. **4b**: Pt1−C1 2.046, Pt1−P1 2.191, Pt1−O1 2.172, Pt1−O2′ 2.108, Pt1−Pt1′ 3.066, O1−Pt1−O2′ 88.8, Pt1−O1−C2 125.9, Pt1−O2′−C2′ 126.0, P1−Pt1−O1−C2 122.7, C1−Pt1−O2′−C2′ −94.2, Pt1−O1−C2−O2 −14.2, Pt1−O2′−C2′−O1′ −5.1. **5b**: Pt1−C1 2.043, Pt1−P1 2.192, Pt1−O1 2.184, Pt1−O2′ 2.117, Pt1−Pt1′ 3.133 O1−Pt1−O2′ 89.2, Pt1−O1−C2 125.9, Pt1−O2′−C2′ 125.5, P1−Pt1−O1−C2 117.0, C1−Pt1−O2′−C2′ −97.9, Pt1−O1−C2−O2 −8.1, Pt1−O2′−C2′−O1′ −5.6.

the fact that only the entropy-favored monomer **2a** is observed in solution. The trifluoroacetate analogues **3b,c** have dimerization energies of about −4 kcal/mol, which is consistent with their observation at low temperature and

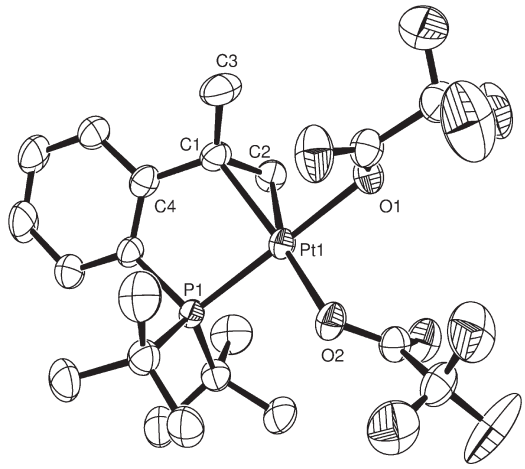

Figure 6. ORTEP representation of the X-ray crystal structure of **6**. Ellipsoids are drawn at 50% probability. Selected distances [Å], angles [deg], and dihedral angles [deg]: Pt1−C1 2.201(5), Pt1−C2 2.093(5), Pt1−P1 2.2488(14), Pt1−O1 2.101(4) Pt1−O2 2.064(4), C1−C2 1.426(8), C1−Pt1−P1 85.47(15), C2−Pt1−C1 95.25(17), C1−Pt1−O1 94.58(19), C2−Pt1−O1 86.2(2), P1−Pt1−O2 94.90(12), O1−Pt1−O2 84.27(16), C2−C1−Pt 66.5(3), C1−C2−Pt 74.8(3), P1−Pt1−C1−C2 −104.2(3), O1−Pt1−C1−C2 78.1(4), C1−C3−C4−C2 −13.8.

the appearance of the monomer **3a** at higher temperatures (vide supra).[31] The sterically unencumbered model compounds **4a** and **5a** are more prone to dimerization (by ca. 9 kcal/mol; see Table 1). This difference originates from the fact that the bulky cyclometalated P-ligand in **2b,c** and **3b,c** induces a severe distortion of the $Pt_2(OOCR)_2$ core as compared to **4b,c** and **5b,c** that bear the carboxylate ligands in the *syn-syn* orientation (Figure 5). This preferable binding mode brings the two platinum centers in relatively close proximity, with Pt−Pt distances ranging from 3.066 to 3.164 Å (Table 1), as was found experimentally for most reported carboxylate-bridged Pt(II) complexes.[19−28] In the sterically crowded complexes **2b,c** and **3c**, a short Pt−Pt contact is made impossible by steric repulsion between the ligands, which accounts for their lower dimerization energies, resulting in the less favorable *syn-skew* binding mode with Pt−Pt distances between 4.606 and 4.714 Å.

From a geometrical point of view, dimer **3b** presents an intermediate case, as the binding mode of the trifluoroacetate ligands is found—both experimentally and computationally—to be in between the *syn-syn* and *syn-skew* coordination mode. This deformation toward the more

(31) Structure **3c** is calculated to be slightly more stable than **3b** (ΔE = 0.25 kcal/mol), in contrast with the observed **3b** as major species at low temperature. However, this energy difference is smaller the generally accepted accuracy of DFT methods, and the relative stability of the two dimers also depends on solvent and temperature effects.

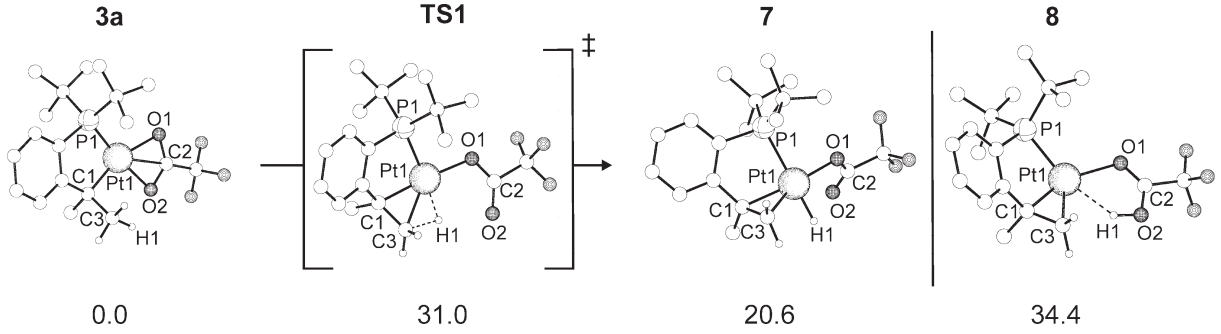

Figure 7. Computed structures and relative energies [kcal/mol] for the complex **3a**, the postulated intermediate **7**, and the transition state that connects them, as well as the hypothetical intermediate **8**. All hydrogen atoms but the ones that are involved in the reaction are excluded for clarity. Selected distances [Å], angles [deg], and dihedral angles [deg]: **3a**: Pt1−C1 2.054, Pt1−P1 2.211, Pt1−O1 2.303, Pt1−O2 2.207, C1−C3 1.559, C3−H1 1.106, C1−Pt1−P1 86.6, C1−Pt1−O2 100.8, O1−Pt1−O2 58.7, P1−Pt1−O1 113.8, Pt1−O1−C2 87.1, Pt1−O2−C2 91.2. **TS1**: Pt1−C1 2.070, Pt1−P1 2.323, Pt1−O1 2.103, Pt1−O2 3.192, Pt1−H1 1.667, C1−C3 1.454, C3−H1 1.588, O2−H1 2.359, C1−Pt1−P1 86.8, C1−Pt1−H1 83.3, C2−Pt1−H1 46.3, P1−Pt1−O1 100.1, Pt1−O1−C2 117.7, O1−Pt1−H1 91.2, P1−Pt1−O1−C2 170.0, C3−C1−Pt1−H1 19.3. **7**: Pt1−C1 2.152, Pt1−P1 2.404, Pt1−O1 2.065, Pt1−H1 1.596, C1−C3 1.418, C1−Pt1−P1 84.1, C1−Pt1−H1 95.8, C2−Pt1−H1 80.1, P1−Pt1−O1 92.5, Pt1−O1−C2 118.0, O1−Pt1−H1 87.0, P1−Pt1−O1−C2 −128.1, C3−C1−Pt1−H1 66.4. **8:** Pt1−C1 2.026, Pt1−P1 2.310, Pt1−O1 2.315, Pt1−H1 2.238, C1−C3 1.458, C1−Pt1−P1 89.6, P1−Pt1−O1 111.7, Pt1−O1−C2 111.9, P1−Pt1−O1−C2 161.3.

Scheme 4

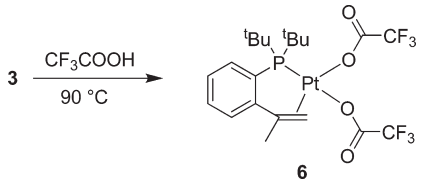

Scheme 5

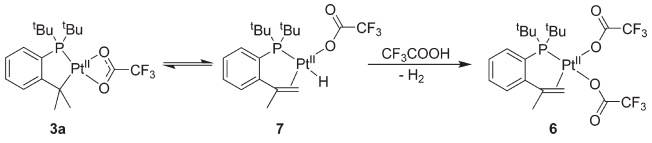

favorable *syn-syn* conformation is accompanied by a strong distortion of the Pt−O−C angles ($\langle\beta\rangle = 132.0°$) compared with the other dimers **2b,c** and **3c** ($\langle\beta\rangle = 122.2$–$124.4°$).

The dimerization of the trifluoroacetate complexes **3a** and **5a** is favored (by ca. 4 kcal/mol; Table 1) over that of the acetate analogues **2a** and **4a**. This observation is independent from the steric encumbrance of the ligand, which suggests it to be a general feature that is highly relevant for catalyst design. One would assume that the electron-poor trifluoroacetate ligands should be preferred over the normal acetates because of their facile interchange of the κ^2- to κ^1-coordination mode (Scheme 1), thereby facilitating the incoming substrate molecules to enter the catalytic cycle. However, our findings indicate that this behavior can be compensated by the higher tendency of the trifluoroacetate complexes to aggregate into the catalytically less active dimers and oligomers.

Ligand Dehydrogenation. When the trifluoroacetate complex **3** was heated in trifluoroacetic acid (TFA) at 90 °C, a facile ligand dehydrogenation was observed affording phosphine-olefin complex **6** (Scheme 4)[32] that was fully characterized by multinuclear NMR spectroscopy and XRD. The crystal structure of **6** reveals a distorted square planar geometry (Figure 6). The olefin is coordinated in an η^2 fashion (Pt1−C1 = 2.201 Å, Pt1−C2 = 2.093 Å) and C1 is slightly pyramidalized (sum of valence angles: 355.4°). The fact that the Pt1−O1 bond (2.101 Å) is longer than Pt−O2 (2.064 Å) indicates that the phosphine ligand has a stronger *trans*-influence than the olefin.

A conceivable mechanism[33] for the formation of **6** consists of a β-hydride elimination affording intermediate **7**, which upon protolysis by trifluoroacetic acid yields bis-acetate **6** (Scheme 5).

Since carboxylate ligands have been shown to act as internal bases in several C−H activation reactions,[10,12] we speculated that this could also facilitate the conversion of **3a**→**6**. To assess the validity of this hypothesis, a transition state (**TS1**) connecting structures **3a** and **7** was optimized using the synchronous transit-guided quasi-Newton (STQN) method[34] (Figure 7). In **TS1**, the Pt−O2 bond is broken, and the transferred hydrogen atom H1 is partially bound to C3 and Pt1 (H1−C3 = 1.588 Å, H1−Pt1 = 1.667 Å). The H1−O2 distance (2.359 Å) is too large for a significant stabilization of the transition state by O−H interaction. In addition, a local minimum was found for the Pt(0) complex [(PCC)Pt(OC(OH)CF_3)] (**8**, PCC = (^{t}Bu$_2$P-*o*-C_6H_4)-C(Me) = CH_2) that would be formed by intramolecular deprotonation of **3a** by the trifluoroacetate ligand, but this Pt(0) complex was calculated to be 3.4 kcal/mol higher in energy than **TS1**, ruling out the base-induced H-abstraction mechanism.

The ligand dehydrogenation reaction described above is related to the one recently reported by Pringle and co-workers,[35] which uses Cl_2 sources as oxidant. The fact

(32) When the reaction was performed in CF_3COOD at 90 °C and monitored by ^{1}H NMR spectroscopy, the isopropenyl moiety of **6** was found to be fully deuterated. This of little mechanistic significance for the conversion of **3** into **6** because the crude product **6** was found to be deuterated within 1 h under the reaction conditions. However, when an analytically pure sample of **6** was used, no H/D exchange was observed under the same conditions, indicating that this process is induced by trace impurities (presumably elemental platinum) in crude **6**.

(33) More complex mechanisms involving traces of elemental platinum cannot be excluded.

(34) Peng, C.; Ayala, P. Y.; Schlegel, H. B.; Frisch, M. J. *J. Comput. Chem.* **1996**, *17*, 49–56.

(35) Baber, A.; Fan, C.; Norman, D. W.; Orpen, A. G.; Pringle, P. G.; Wingad, R. L. *Organometallics* **2008**, *27*, 5906–5910.

that TFA as strong Brønsted acid can be used instead opens interesting perspectives for alkane functionalization because strongly coordinating anions such as Cl^- would likely prevent the formation of the C−H σ-complex that is a necessary intermediate for C−H activation.[36] In related work, the use of N-donor ligands has allowed the observation of intramolecular[37,38] and intermolecular[36,39] alkane dehydrogenation reactions resulting in olefin hydride complexes comparable to intermediate **7**. The observation that the treatment of **3a** with a strong acid results in a dehydrogenation reaction rather than in the protolysis of the Pt−C bond suggests that a strongly acidic, weakly coordinating medium like trifluoroacetic acid should be suitable for platinum-catalyzed dehydrogenation of alkanes, which is currently under active investigation.

Conclusions. The use of a bulky, anionic P,C-donor ligand allowed the preparation of a rare, monomeric platinum(II) κ^2-acetate complex and its trifluoroacetate analogue. The latter crystallizes as a strained dimer, but exists in solution as a mixture of two isomeric dimers and the monomer. DFT calculations confirmed that the dimers were destabilized by steric repulsion between the ligands. Additionally, both the experimental and computational results indicate that trifluoroacetate ligands tend to favor dimeric structures more than acetate ligands. Finally, an acceptor-free ligand-dehydrogenation reaction was found to take place in hot trifluoroacetic acid. DFT investigations showed that this reaction could proceed via a concerted β-elimination with a change in the coordination mode of the trifluoroacetate ligand from κ^2 to κ^1.

Experimental Part

General Procedures. Solvents were distilled under nitrogen over sodium (hexane) sodium/potassium (diethylether), CaH_2 (isopropanol, dichloromethane). All chemical manipulations involving metal complexes were performed under an inert atmosphere using standard Schlenk and glovebox techniques unless stated otherwise. ^{1}H and ^{13}C chemical shifts are reported in ppm relative to tetramethylsilane, using residual solvent proton and ^{13}C resonance as internal standard. ^{19}F and ^{31}P chemical shifts are reported in parts per million relative to $CFCl_3$ and 85% aqueous H_3PO_4 used as external standards. Multiplicities are indicated s (singlet), d (doublet), t (triplet), dd (doublet doublet), d sept (doublet of septets) while apparent singlets, doublets, and triplets are indicated by "s", "d", and "t", respectively. In cases where an unambiguous assignment of the individual peaks in ^{13}C NMR spectra was not possible, the possible assignments are separated by "/".

Elemental analyses were carried at the Mikrolabor of the Laboratorium für Organische Chemie of ETH Zürich. Organolithium reagents were titrated using the procedure from Watson and Eastham.[40] $[(PhCN)_2PtCl_2]$[41] was prepared according to a literature procedure. $(^tBu)_2(^iPr)P$[29] and complex **1**[29] were synthesized by modified literature procedures. All other chemicals were obtained commercially and used as received.

(2-Isopropylphenyl)-di-*tert*-butylphosphine. An 1.7 M solution of *tert*-butyllithium in pentane (5.0 mL, 8.5 mmol) was added dropwise to a 0 °C solution of 1-bromo-2-isopropylbenzene (1.59 g, 8.0 mmol) in diethylether (16 mL), and the resulting mixture was stirred for 20 min at 0 °C. Di-*tert*-butylphosphinechloride (1.29 g, 6.8 mmol) was then slowly added, and the resulting solution was refluxed for 48 h, after which N_2-purged water (10 mL) was added. The organic phase was concentrated under reduced pressure, and the residue was heated at 100 °C for 30 min at 25 mbar to remove the volatile impurities, affording the crude product as a yellowish oil (1.48 g, 82%) that was used without further purification for complex syntheses. ^{1}H NMR (300 MHz, $CDCl_3$): δ 7.70 (d, ^3J(H−H) = 7.8 Hz, 1H, Ar*H*), 7.35−7.25 (m, 2H, Ar*H*), 7.16−7.09 (m, 1H, Ar*H*), 4.31 (d sept, ^3J(H−H) = 6.9 Hz, ^4J(H−^{31}P) = 10.2 Hz, 1H, ArC*H*$(CH_3)_2$), 1.20 (d, ^3J(H−^{31}P) = 12.0 Hz, 18H, PCC*H*$_3$), 1.20 (d, ^3J(H−H) = 6.9 Hz, 6H, ArCH(C*H*$_3)_2$). ^{31}P{^{1}H} NMR (121 MHz, $CDCl_3$): δ 13.2.

$[(PC)Pt(\mu\text{-}Cl)]_2$ (1). (2-Isopropylphenyl)-di-*tert*-butylphosphine (529 mg, 2.0 mmol) was added to a stirred suspension of $[(PhCN)_2PtCl_2]$ (944 mg, 2.0 mmol) and 1,2,2,5,5-pentamethylpiperidine (365 μL, 2.0 mmol) in isopropanol (32 mL), and the mixture was refluxed for 24 h. The resulting brownish precipitate was collected by filtration and washed with diethylether (3 × 20 mL). Traces of elemental platinum were removed by dissolution of the solid in dichloromethane and filtration over Celite. Removal of the solvent under reduced pressure and drying in vacuo afforded the product as a white solid (470 mg, 47.5%). An analytically pure sample was obtained by vapor diffusion of hexane into a solution of **1** in dichloromethane/hexane. The NMR data indicates that a mixture of two isomers **1a/b** and **1b/a** exist in a 3:2 ratio in solution. ^{1}H NMR (300 MHz, CD_2Cl_2): isomer **1a/b**: δ 7.59−7.51 (m, 1H, Ar*H*), 7.49−7.43 (m, 1H, Ar*H*), 7.35−7.26 (m, 1H, Ar*H*), 7.22−7.14 (m, 1H, Ar*H*), 1.56 (s, ^3J(H−^{195}Pt) = 40 Hz, 6H, PtCC*H*$_3$), 1.46 (d, ^3J(H−^{31}P) = 14.3 Hz, 18H, PCC*H*$_3$). Isomer **1b/a**: δ 7.59−7.51 (m, 1H, Ar*H*), 7.49−7.43 (m, 1H, Ar*H*), 7.35−7.26 (m, 1H, Ar*H*), 7.22−7.14 (m, 1H, Ar*H*), 1.58 (s, ^3J(H−^{195}Pt) = 37 Hz, 6H, PtCC*H*$_3$), 1.43 (d, ^3J(H−^{31}P) = 14.3 Hz, 18H, PCC*H*$_3$). ^{13}C{^{1}H} NMR (75 MHz, CD_2Cl_2): Isomers **1a** + **1b** δ 132.7 (C_{Ar}), 132.19 (C_{Ar}), 132.15 (C_{Ar}), 132.0 (C_{Ar}), 131.1 (C_{Ar}), 126.0 (C_{Ar}), 125.9 (C_{Ar}), 125.8 (C_{Ar}), 125.6 (C_{Ar}), 37.6 (^1J(C−^{31}P) = 28.6 Hz, P*C*$(CH_3)_3$), 37.5 (^1J(C−^{31}P) = 28.8 Hz, P*C*$(CH_3)_3$), 36.1 (Pt*C*), 35.9 (Pt*C*), 34.9 (PtC*C*H$_3$), 34.4 (PtC*C*H$_3$), 30.53 (^4J(H−^{195}Pt) = ∼26 Hz, PC*C*H$_3$), 30.48 (^4J(H−^{195}Pt) = ∼26 Hz, PC*C*H$_3$). ^{31}P{^{1}H} NMR (121 MHz, $CDCl_3$): δ 69.7 (s, ^1J(P−^{195}Pt) = 5.31 kHz, isomer **1a/b**), 69.6 (s, ^1J(P−^{195}Pt) = 5.37 kHz, isomer **1b/a**). Anal.: calcd for $C_{34}H_{56}P_2Cl_2Pt_2$ C 41.34, H 5.71. Found C 41.41, H 5.71.

$[(PC)Pt(\kappa^2\text{-}O_2CCH_3)]$ (2a). AgOAc (18 mg, 108 μmol) was added to a solution of **1** (53 mg, 54 μmol) in dichloromethane (1.5 mL) and stirred for 30 s, during which time a white precipitate (AgCl) formed. Filtration, evaporation of the solvent, and drying in vacuo afforded the product as a colorless solid (44 mg, 79%). An analytically pure sample was obtained by slow concentration of a solution of **2a** in hexane. M.p.: 133−139 °C. ^{1}H NMR (300 MHz, CD_2Cl_2): δ 7.52−7.42 (m, 2H, Ar*H*), 7.35−7.28 (m, 1H, Ar*H*), 7.23−7.16 (m, 1H, Ar*H*), 1.95 (s, 3H, O_2CCH_3), 1.40 (d, ^3J(H−^{31}P) = 14.3 Hz, 18H, PCC*H*$_3$), 1.38 (s, ^3J(H−^{195}Pt) = 35 Hz, 6H, PtCC*H*$_3$). ^{13}C{^{1}H} NMR (75 MHz, DEPT(90, 135), CD_2Cl_2): δ 189.0 (d, ^3J(C−^{31}P) = 3.2 Hz, O*C*C), 168.3 (d, ^2J(C−^{31}P) = 23.5 Hz, $C_{Ar}{}^2$), 133.0 (d, ^1J(C−^{31}P) = 51.3 Hz, $C_{Ar}{}^1$), 131.6 (d, CH, J(C−^{31}P) = 3.0 Hz, $C_{Ar}{}^{3/4/5}$), 131.4 (d, CH, J(C−^{31}P) = 2.5 Hz, $C_{Ar}{}^{3/4/5}$), 126.7 (d, CH, ^3J(C−^{31}P) = 7.4 Hz, $C_{Ar}{}^{3/5}$), 125.2 (d, CH, ^2J(C−^{31}P) = 15.5 Hz, $C_{Ar}{}^6$), 37.1 (d, ^1J(C−^{31}P) = 31.0 Hz, P*C*$(CH_3)_3$), 32.4 (d, CH_3, ^3J(C−^{31}P) = 1.7 Hz, ^2J(C−^{195}Pt) = ∼40 Hz (br Pt sattelites), PtC*C*H$_3$), 30.1 (d, CH_3, ^2J(C−^{31}P) = 4.1 Hz, ^2J(C−^{195}Pt) = 31 Hz, PC*C*H$_3$), 29.1 (d, ^2J(C−^{31}P) = 0.8 Hz,

(36) Chen, G. S.; Labinger, J. A.; Bercaw, J. E. *Proc. Natl. Acad. Sci. U.S. A.* **2007**, *104*, 6915–6920.
(37) Fekl, U.; Goldberg, K. I. *J. Am. Chem. Soc.* **2002**, *124*, 6804–6805.
(38) Kloek, S. M.; Goldberg, K. I. *J. Am. Chem. Soc.* **2007**, *129*, 3460–3461.
(39) West, N. M.; White, P. S.; Templeton, J. L. *Organometallics* **2008**, *27*, 5252–5262.
(40) Watson, S. C.; Eastham, J. F. *J. Organomet. Chem.* **1967**, *9*, 165–168.
(41) Anderson, G. K.; Lin, M. *Inorg. Synth.* **1990**, *28*, 60–63.

^1J(C−^{195}Pt) not resolved, Pt*C*), 25.7 (d, CH_3, ^4J(C−^{31}P) = 2.8 Hz, OOC*C*H$_3$). ^{31}P{^{1}H} NMR (121 MHz, CD_2Cl_2): δ 71.2 (s, ^1J(P−^{195}Pt) = 5.15 kHz). Anal.: calcd for $C_{19}H_{31}O_2PPt$ C 44.10, H 6.04. Found C 43.58, H 6.02. Crystals suitable for XRD were obtained by slow concentration of a solution of **2a** in hexane.

[(PC)Pt(O$_2$CCF$_3$)]$_2$ (3). AgO_2CCF_3 (40 mg, 182 μmol) was added to a solution of **1** (90 mg, 91 μmol) in dichloromethane (4 mL) and stirred for 30 s, during which time a white precipitate (AgCl) formed. Filtration, evaporation of the solvent, and drying in vacuo afforded the product as a colorless solid (81 mg, 77%). ^{1}H NMR (300 MHz, CD_2Cl_2), 21 °C (**3a** ⇄ **3b** ⇄ **3c**): δ 7.55−7.42 (m, 2H, Ar*H*), 7.38−7.28 (br, 1H, Ar*H*), 7.28−7.16 (br, 1H, Ar*H*), 1.43 (br "d", 24H, ^3J(H−^{31}P) = 14.5 Hz, PCC*H*$_3$ + PtCC*H*$_3$). −50 °C (**3b**⇄**3c**): δ 7.53−7.38 (m, 2H, Ar*H*), 7.33−7.25 (m, 1H, Ar*H*), 7.22−7.14 (m, 1H, Ar*H*), 1.43, 1.40, 1.38, 1.36, 1.33, 1.32, 1.28, 1.12 (24H, C*H*$_3$). ^{19}F{^{1}H} NMR (282 MHz, CD_2Cl_2), 21 °C: δ −74.5 (br, **3b**), −74.8 (v br, **3a**). −50 °C: δ −74.1 (s, 4.7%, **3c**), −74.3 (s, 85%, **3b**), −74.6 (s, 4.7%, **3c**) − 75.4 (s, 5.9%). ^{31}P{^{1}H} NMR (121 MHz, CD_2Cl_2), 21 °C: δ 72.8 (v br, **3a**), 66.4 (br, **3b**), ^1J(P−^{195}Pt) not resolved. −30 °C: δ 66.2 (12%, ^1J(P−^{195}Pt) not resolved, **3c**), 65.9 (88%, ^1J(P−^{195}Pt) = 5.60 kHz, **3b**). Anal.: calcd for $C_{19}H_{28}O_2F_3PPt$ C 39.93, H 4.94. Found C 39.95, H 4.83. Suitable crystals (M.p.: ≥ 210 °C (dec.)) of **3b** for XRD were obtained by vapor diffusion of hexane into a solution of **3** in dichloromethane/hexane.

[(PCC)Pt(O$_2$CCF$_3$)$_2$] (6). A solution of **3** (52 mg, 91 μmol) in trifluoroacetic acid (5 mL) was heated at 90 °C for 17 h. The solvent was evaporated in vacuo, and the crude product was taken into dichloromethane (1 mL). A small amount of black precipitate (presumably Pt(0)) was removed by filtration, and the solution was layered with hexane (4 mL). After 2 days, a small amount of product had crystallized, and the crystallization was completed by vapor diffusion of hexane into the mixture. Filtration, washing with hexane (4 × 1 mL) and drying in vacuo afforded the product as colorless crystals (27 mg, 40%). M.p.: ≥ 190 °C (dec.) °C. ^{1}H NMR (300 MHz, CD_2Cl_2): δ 7.67−7.47 (m, 4H, Ar*H*), 4.62 (s, ^2J(H−^{195}Pt) = 70.0 Hz, 1H, C=C*H*), 3.70 (s, ^2J(H−^{195}Pt) = 58.8 Hz, 1H, C=C*H*), 2.39 (s, ^3J(H−^{195}Pt) = 40.4 Hz, 3H, PtCC*H*$_3$), 1.53 (d, ^3J(H−^{31}P) = 15.8 Hz, 9H, PC(C*H*$_3$)$_3$), 1.44 (d, ^3J(H−^{31}P) = 15.8 Hz, 9H, PC(C*H*$_3$)$_3$). ^{13}C{^{1}H} NMR (75 MHz, DEPT(90, 135), CD_2Cl_2): δ 153.1 (d, ^2J(C−^{31}P) = 13.7 Hz, C_{Ar}^2), 134.2 (d, CH, J(C−^{31}P) = 2.7 Hz, $C_{Ar}^{3/4/5}$), 133.5 (d, CH, J(C−^{31}P) = 2.6 Hz, $C_{Ar}^{3/4/5}$), 129.6 (d, CH, ^3J(C−^{31}P) = 8.0 Hz, $C_{Ar}^{3/5}$), 126.8 (d, CH, ^2J(C−^{31}P) = 11.6 Hz, C_{Ar}^6), 125.2 (d, ^1J(C−^{31}P) = 51.8 Hz, C_{Ar}^1), 109.6 (d, ^3J(C−^{31}P) = 4.6 Hz, Ar*C* = CH$_2$), 73.1 (d, CH$_2$, ^4J(C−^{31}P) = 1.1 Hz, ArC = *C*H$_2$), 38.5 (d, ^1J(C−^{31}P) = 27.8 Hz, P*C*(CH$_3$)$_3$), 37.9 (d, ^1J(C−^{31}P) = 26.0 Hz, P*C*(CH$_3$)$_3$), 30.0 (d, CH$_3$, ^2J(C−^{31}P) = 2.8 Hz, PC*C*H$_3$), 29.5 (d, CH$_3$, ^2J(C−^{31}P) = 2.6 Hz, PC*C*H$_3$), 23.4 (s, CH$_3$, ArC*C*H$_3$). No ^{13}C NMR signals were observed for the CF_3CO_2 units, presumably because of depletion of the signal intensity by C−^{19}F coupling. ^{19}F{^{1}H} NMR (282 MHz, CD_2Cl_2): δ −74.5 (s, C*F*$_3$), −74.8 (s, C*F*$_3$). ^{31}P{^{1}H} NMR (121 MHz, CD_2Cl_2): δ 55.7 (s, ^1J(P−^{195}Pt) = 3.45 kHz). Anal.: calcd for $C_{21}H_{27}O_4F_6PPt$ C 36.90, H 3.98. Found C 36.95, H 3.84. Crystals suitable for XRD were obtained by vapor diffusion of hexane into a solution of **6** in dichloromethane/hexane.

X-ray Crystallography. Relevant details about the structure refinements are given in Table 2, and selected geometrical parameters are included in the captions of the corresponding figures. Data collection was performed on a Bruker-Nonius Kappa-CCD (graphite monochromator, Mo Kα). The structure was solved by direct methods[42] and refined by full-matrix least-squares analysis[43] including an isotropic extinction correction. All non H-atoms were refined anisotropically (H-atoms isotropic, whereby H-positions are based on stereochemical considerations).

Table 2. Crystallographic Data for Compounds **2a**, **3b**, and **6**

	2a	**3b**	**6**
chem formula	$C_{19}H_{31}O_2PPt$	$C_{38}H_{56}F_6O_4P_2Pt_2$	$C_{21}H_{27}F_6O_4PPt$
fw	517.5	1143.0	683.5
cryst syst	monoclinic	monoclinic	monoclinic
space group	*P*21/*c*	*P*21/*c*	*P*21/*n*
a [Å]	8.1056(1)	9.7931(2)	10.8654(3)
b [Å]	8.6165(2)	26.3620(5)	15.9547(6)
c [Å]	29.1594(6)	16.3319(4)	14.0385(4)
α [deg]	90	90	90
β [deg]	95.310(1)	98.0311(10)	95.003(2)
γ [deg]	90	90	90
V [Å^3]	2027.81(7)	4175.0(2)	2424.36(13)
Z	4	4	4
D_{calcd} [g cm^{-3}]	1.695	1.818	1.873
F(000)	1016	2224	1328
μ [mm^{-1}]	7.005	6.834	5.924
temp. [K]	220	223	220
wavelength [Å]	0.7107	0.7107	0.7107
measd rflns	7647	23104	9541
unique rflns	4633	8435	5511
data/restraints/param	4633/0/218	8435/0/469	5511/0/310
$R(F)$ ($I > 2\sigma(I)$)	0.0342	0.0591	0.0363
$wR(F^2)$ ($I > 2\sigma(I)$)	0.0986	0.1624	0.0815
GOF	1.030	1.172	0.940

Computational Methods. All DFT calculations were performed using Gaussian 03.[44] Geometry optimizations were performed using the Becke three parameters hybrid functional[45] using the Perdew−Wang[46] non-local correlation. The Stuttgart/Dresden[47,48] basis set and effective core potential were used for Pt, along with a 6-31G(d) basis set on all other atoms. A frequency calculation was performed on all converged geometries to verify that they were minima.

Transition states were computed using the QST3 (Synchronous Transit-Guided Quasi-Newton) method.[34] A subsequent frequency calculation was used to check that the converged geometries were first order saddle points, and that the only negative frequency corresponded to the desired reaction coordinate.

All energies were ZPE corrected using a scaling factor of 0.9774 as proposed by Scott and Radom[49] for B3PW91/6-31G(d).

Acknowledgment. The authors acknowledge support from the Swiss National Foundation. A TALENT stipend (J.C.S.) of The Netherlands Organization for Scientific Research (NWO) is gratefully acknowledged. We thank Dr. B. Schweizer and Mr. P. Seiler for the X-ray structure determinations.

Supporting Information Available: XRD data in cif format, figures representing the computed structures for **2a**−**5a** and **2c**−**5c**, computed coordinates and frequencies for all structures, full reference 44. This material is available free of charge via the Internet at http://pubs.acs.org.

(42) Altomare, A.; Burla, M.; Camalli, M.; Cascarano, G.; Giacovazzo, C.; Guagliardi, A.; Moliterni, A.; Polidori, G.; Spagna, R. *J. Appl. Crystallogr.* **1999**, *32*, 115–119.

(43) Sheldrick, G.M.; *SHELXL-97 Program for the Refinement of Crystal Structures*; University of Göttingen: Göttingen, Germany, 1997.

(44) Frisch, M. J. et al. *Gaussian 03*, Revision D.01; Gaussian, Inc.: Wallingford, CT, 2004.

(45) Becke, A. D. *J. Chem. Phys.* **1993**, *98*, 5648.

(46) Perdew, J. P.; Burke, K.; Wang, Y. *Phys. Rev. B* **1996**, *54*, 16533.

(47) Bergner, A.; Dolg, M.; Kuechle, W.; Stoll, H.; Preuss, H. *Mol. Phys.* **1993**, *80*, 1431.

(48) Dolg, M.; Stoll, H.; Preuss, H.; Pitzer, R. M. *J. Phys. Chem.* **1993**, *97*, 5852.

(49) Scott, A. P.; Radom, L. *J. Phys. Chem.* **1996**, *100*, 16502–16513.